Vol. 19, e190020 (2022)
doi: 10.2142/biophysico.bppb-v19.0020

Biophysics and Physicobiology
https://www.jstage.jst.go.jp/browse/biophysico/

Review Article (Invited)

Exploring order in active turbulence: Geometric rule and pairing order transition in confined bacterial vortices

Kazusa Beppu, Yusuke T. Maeda

Department of Physics, Kyushu University, Fukuoka 819-0395, Japan

Received April 6, 2022; Accepted May 10, 2022;
Released online in J-STAGE as advance publication May 12, 2022
Edited by Takeharu Nagai

Ordered collective motion emerges in a group of autonomously motile elements (known as active matter) as their density increases. Microswimmers, such as swimming bacteria, have been extensively studied in physics and biology. A dense suspension of bacteria forms seemingly chaotic turbulence in viscous fluids. Interestingly, this active turbulence driven by bacteria can form a hidden ensemble of many vortices. Understanding the active turbulence in a bacterial suspension can provide physical principles for pattern formation and insight into the instability underlying biological phenomena. This review presents recent findings regarding ordered structures causing active turbulence and discusses a physical approach for controlling active turbulence via geometric confinement. When the active matter is confined in a compartment with a size comparable to the correlation length of the collective motion, vortex-like rotation appears, and the vortex pairing order is indicated by the patterns of interacting vortices. Additionally, we outline the design principle for controlling collective motions via the geometric rule of the vortex pairing, which may advance engineering microdevices driven by a group of active matter. This article is an extended version of the Japanese article, Ordered Structure and Geometric Control of Active Matter in Dense Bacterial Suspensions, published in SEIBUTSU BUTSURI Vol. 60, p.13-18 (2020).

Key words: active matter, bacterial suspensions, chirality, edge current

Significance

"Active matter" refers to a class of materials that move autonomously by consuming chemical energy and form an ordered flocking cluster or exhibit a complex turbulent state at a high density. The physics of active matter provides a new foundation for understanding the self-organization of complex biological systems at different scales, including proteins, bacteria, and multicellular tissues. This review outlines the emergent order of vortices hidden in an active turbulent state and provides a simple geometric rule in which the geometry of vortex pairings plays an important role in controlling the collective motion of active matter.

Introduction

In nature, one often sees birds, fish, and other elements move on their own, often in groups [1]. Similarly, at the microscale, cells—which are the building blocks of individual organisms—move and grow while forming an ordered structure during morphogenesis. At the nanoscale, motor proteins in a living cell convert chemical energy into autonomous motion fueled by adenosine triphosphate (ATP) hydrolysis. Highly ordered structures regulated by actively moving elements are commonly observed in nature, including molecules, cells, and individual animals [2]. Materials or cells that move by self-propelling and exhibit highly correlated motion are known as active matter. The physics of active matter is

Corresponding author: Yusuke T. Maeda, Department of Physics, Kyushu University, 744 Motooka, Nishi-ku, Fukuoka 819-0395, Japan. ORCID iD: https://orcid.org/0000-0001-7848-7654, e-mail: ymaeda@phys.kyushu-u.ac.jp

an emerging field that bridges the gap between physics and biology from the perspective of ordered collective dynamics [3].

In 1995, Vicsek et al. developed a theoretical model of self-propelled particles that considers autonomous motion at a constant speed and the interaction among particles aligning their orientation of motion [4]. In this theoretical model, there is an effect by which particles try to align their orientation when they are close together, but they are not perfectly aligned due to noise. When the noise level is low, collective motion is realized, in which the particles are oriented toward each other. As the noise increases, a disordered state appears in which the particles exhibit random motion. Using the Vicsek model, the collective motion of active matter can be analyzed within the framework of phase transitions. The model provides rich theoretical and experimental frameworks that are essential for understanding various biological phenomena.

A group of active matter, such as swimming bacteria [5,6], sperm cells [7], eukaryotic cells [8,9], or the complex of motor proteins and cytoskeletons [10], exhibits a variety of dynamic ordered structures, such as swarming, flocking, and vortex lattices, as well as synthetic systems, such as assemblies of colloids or robots [1–4]. Numerous ordered patterns are still being discovered and have been extensively studied in non-equilibrium physics; one fascinating example is the active turbulence of dense bacterial suspensions. The bacteria most commonly used in studies on active turbulence are *Escherichia coli* (*E.coli*) and *Bacillus subtilis* (*B. subtilis*), which have rod-shaped bodies with multiple flagella. These swimming bacteria align their directions of motion with each other as their density increases because of the excluded volume effect, which makes the front–back axes of the rods parallel to each other. In addition, the bacterial body generates a pusher-type force dipole in the surrounding fluid owing to the rotation of the flagella. The emergent force dipole exerts the stress driving water flow, and the long-range hydrodynamic interaction between the bacteria (the force dipoles) prevents the steric effect from aligning the bacteria in the same direction in a quasi-two-dimensional space. As the effect of the polar aligning interaction decays over long distances, a turbulent state appears in the aligned direction at short distances, but disordered motion occurs at longer distances (Fig. 1). This is reminiscent of classical turbulent flows with high Reynolds numbers, i.e., Re >> 1, despite active turbulence occurring at low Reynolds numbers (Re ≈ 10^{-5}), rendering the fluid inertia negligible. The key difference between active and classical turbulences is the manner in which the injected energy cascades over scales. In inertial turbulence, the energy injection is determined by external driving, whereas the energy input in active turbulence is from bacterial swimming, which self-organize into correlated structures at larger scales [11] (Fig. 1).

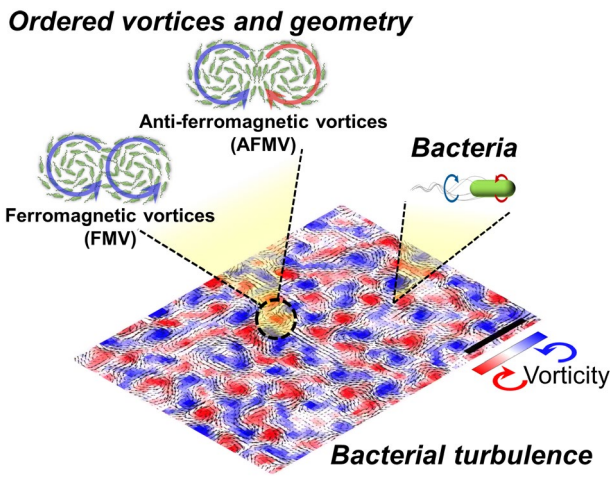

Figure 1 Bacterial turbulence and ordered interacting vortices. Bacterial turbulence consists of mesoscale vortices of CW (red domain in vorticity) and CCW (blue domain). Vortex pairing patterns of ferromagnetic vortices (FMV) and anti-ferromagnetic vortices (AFMV) can be found. Scale bar is 100 μm.

By examining the velocity correlations in this turbulent state, Wensink et al. found that during turbulence, the velocity field has a correlation length with a characteristic size, that is, numerous vortices are embedded in the spatial structure [12]. The characteristic lengths exhibiting this vortex structure can be reproduced using a continuum model of collective motion, which assumes an instability that prevents the formation of long-wavelength structures. Intriguingly, Wioland et al. demonstrated that a single vortex of bacteria can be extracted by designing a circular boundary shape using water-in-oil droplets. These droplets had radii comparable to the characteristic length of the bacterial velocity correlation [13]. This finding indicates that the vortical motion becomes stable when it interacts with the circular wall, and geometric confinement with a characteristic length scale unveils the hidden order of the constituent vortices inherent in active turbulence. However, while the collective motion of bacteria is an experimental model to explore the collective motion of active matter, it is known that the Vicsek model does not exhibit order formation at intermediate scales, such as vortex patterns. Therefore, various studies have been conducted for clarifying the physical characteristics of the vortex motion with the aim of revealing in what respects the collective motion exhibited by bacteria is consistent with the conventional Vicsek model and in what respects it requires a new theoretical interpretation.

Geometric Control of Collective Motion in Dense Bacterial Suspensions

Bacterial turbulence comprises numerous mesoscale interacting vortices, such as the co-rotational pairing of two vortices

rotating in the same direction and the anti-rotational pairing of two vortices rotating in opposite directions. The ordered structure of a vortex has two degrees of freedom: counterclockwise (CCW) and clockwise (CW) rotation directions. The pattern of interacting vortices is determined by their coupling, i.e., whether they are oriented in the same direction or opposite directions. This concept is similar to the spin orientation of interacting electrons in condensed-matter physics; the CCW or CW vortex is regarded as spin up or spin down in the context of condensed-matter physics, and in the same manner, the co-rotational (or anti-rotational) pairing of vortices is called "ferromagnetic" (or "antiferromagnetic") (Figs. 2A and B). In a simple model of interacting spins, the state in which multiple interacting spins are oriented in an orderly manner is called the ferromagnetic phase. The ferromagnetic phase is in a state of global order, with aligned spin orientations in the same direction. In contrast, a state in which the direction of the spins is reversed from that of the neighboring spins is called an antiferromagnetic phase. Thus, by comparing the rotation of vortices in the direction of

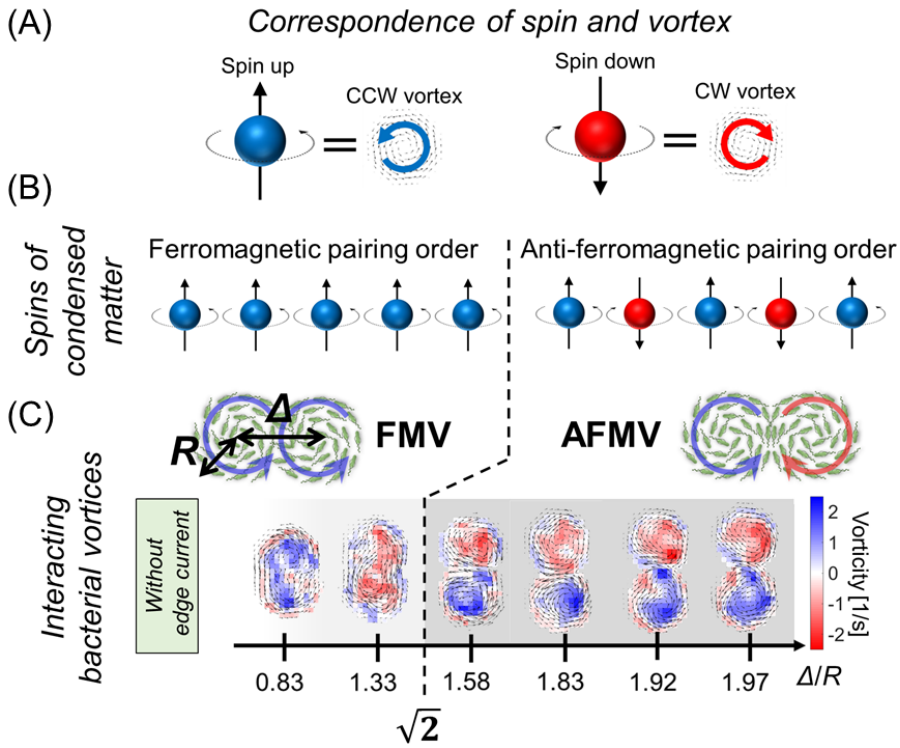

Figure 2 Vortex order and vortex pairing transition in confined bacterial turbulence. (A) Correspondence of spin (up and down) and bacterial vortex (CCW and CW). (B) Correspondence of ordered spins and ordered vortices. (C) Geometry dependence of vortex pairings (FMV and AFMV) in microwells with the symmetric interface. The dashed line at $\Delta_c/R = \sqrt{2}$ is the transition point of pairing order transition between FMV and AFMV. Colors code vorticity. This figure is modified from [16].

spins, the analogy of condensed-matter physics can be used to study the self-organization of interacting active vortices.

Wioland et al. built a microfluidic device in which a bacterial suspension is enclosed via geometric confinement. Bacterial vortices arise from collective motion under confinement and interact with each other by arranging themselves in a square lattice [14]. Bacteria can swim through microchannels placed between the confined bacterial vortices. By changing the microchannel width, the interaction of bacterial vortices can be controlled. Interestingly, two ordered patterns of interacting bacterial vortices appeared in this device: a ferromagnetic vortex (FMV) pattern, in which the vortices exhibited the same direction of rotation, and an antiferromagnetic vortex (AFMV) pattern, in which neighboring vortices were oriented in opposite directions. The FMV pattern appeared when the channel width was sufficient, indicating that the vortex pairing patterns in the lattice-like microfluidic device are geometry-dependent. Furthermore, Nishiguchi et al. reported that by installing pillars at regular spacing in bacterial turbulence, the turbulent dynamics can be transformed into a lattice of AFMV patterns, despite the small volume occupied by the pillars [15]. From a macroscopic viewpoint, active turbulence holds symmetry in that the global vorticity should always be zero, implying the presence of robust antiferromagnetic vortices. Although it has been clarified that co-rotating and anti-rotating ordered vortices can be controlled by changing the geometry, little was known about the physical principle underlying this geometric control until recently.

To this end, Beppu et al. developed a new microwell that allowed two bacterial vortices to interact [16]. This study focused on two geometric quantities of the constituent ordered vortices (the radius of the vortices R and the distance between vortices Δ), and their geometric rule was revealed (Figs. 2C and 3). The RP4979 strain of *E. coli* that exhibits smooth swimming without tumbling is enclosed in double-circular microwells at a density (volume fraction) of ~20 v/v%. The dimensionless parameter Δ/R defines this double-circular geometry. Intriguingly, both FMV-like vortex pairing and AFMV-like vortex pairing emerge, but they depend on Δ/R, as indicated by the transition of the FMV to an AFMV at the critical point $\Delta_c/R \approx 1.4$ (in Fig. 2C).

To understand the pairing-order transition from the FMV to the AFMV, a theoretical model based on the Vicsek model is considered with a confinement boundary condition [4]. The position of the m^{th} particle is $\mathbf{r_m} = \big(x_m(t), y_m(t)\big)$ with radial distance r_m and orientation $\boldsymbol{d}\big(\theta_m(t)\big) = (\cos\theta_m(t), \sin\theta_m(t))$. The orientational dynamics is given as

$$\dot{\theta}_m = -\overline{\gamma_p} \sum_{r_{mn}<\varepsilon} \sin(\theta_m - \theta_n) + \eta_m(t), \tag{1}$$

where $\overline{\gamma_p}$ is the coefficient of polar alignment among the particles, $r_{mn} = |r_m - r_n|$ represents the distance between the m^{th} and n^{th} particles, ε represents the effective radius of polar interactions (Fig. 3A, left), and η_m represents white Gaussian noise that satisfies $\langle\eta_m\rangle = 0$ and $\langle\eta_m(t)\eta_n(t')\rangle = 2D\delta_{mn}\delta(t-t')$, with D denoting the rotational diffusion coefficient, δ_{mn} denoting the Kronecker delta function, and $\delta(t-t')$ denoting the Dirac delta function. The emergent patterns are determined by the resulting orientation of bacteria interacting at the tip, where the two circles intersect (Fig. 3C). The orientation of bacteria going or coming from the tip (characterized by Ψ) is constrained in the tangential direction. Therefore, by considering the geometry of the tip and taking the mean-field approximation for the summation (Fig. 3C), we can obtain the effective potential of the FMV and AFMV: ${U_p}^{FMV} = -\gamma_p \sin\Psi$ at $\theta = 0$ for the FMV, and ${U_p}^{AFMV} = -\gamma_p \cos\Psi$ at $\theta = \pi/2$ for the AFMV (note that we set $\gamma_p = \sum_{r_{mn}<\varepsilon} \overline{\gamma_p}$). ${U_p}^{FMV} = {U_p}^{AFMV}$ gives a transition point $\Delta_c/R = \sqrt{2}$, which is consistent with the experimental results. This geometric rule corresponds to the case with the tip angle $2\Psi = \pi/2$ at which there is no preference between the FMV and the AFMV, leading to the transition point (Fig. 3C), which suggests that ordered interacting vortices of bacteria have symmetric polar interactions.

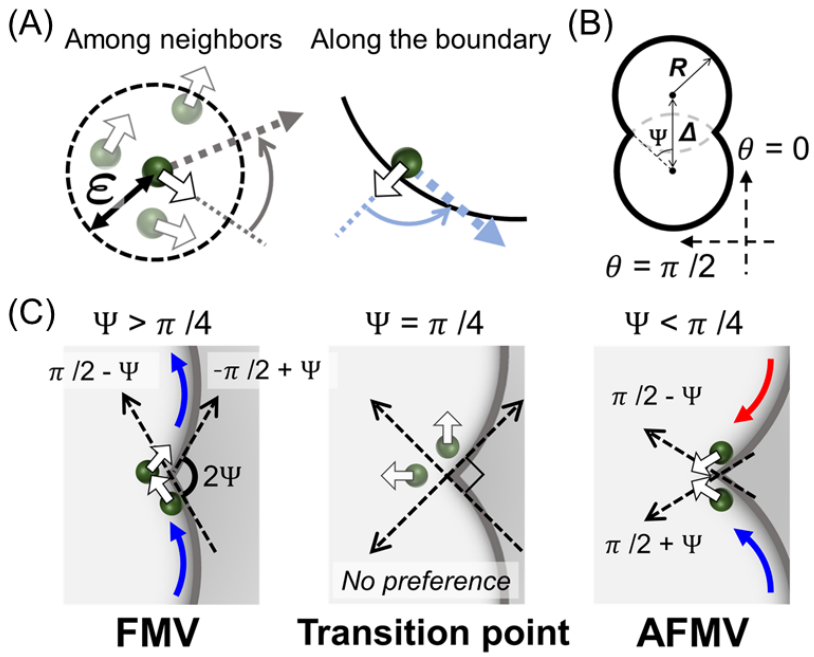

Figure 3 Theoretical interpretation of vortex pairing transition. (A) Polar alignment of heading angle among neighboring particles (left) and nematic alignment along the wall (right). (B) Definition of doublet circular boundary and setting angle. (C) Polar interaction around a tip defined by Ψ. FMV is preferred when Ψ>π/4 (left), while AFMV is preferred when Ψ<π/4 (right). Colliding at Ψ=π/4 exhibits no preference in the resulting patterns. This figure is modified from [16].

Controlling Chiral Active Matter

A strategy to control active turbulence is crucial for understanding the onset of active turbulence and for developing a novel route to efficiently harvest energy from turbulent-like disordered motions. Although the simple geometric quantity Δ/R can be used to control interacting ordered vortices, it is unclear how ordered vortices with a net circulation over scales far larger than the correlation length can be controlled. One strategy is to use the viscoelastic properties of the ambient environment to suppress the decay of directional correlations, which has been reported to achieve large bacterial vortices with sizes of several hundred micrometers [17]. However, the bacteria also have properties that affect the velocity correlations, which have long been overlooked. One of these properties is chirality, that is, the mirror-symmetry breaking of individual units. Chirality is ubiquitous; examples include amino acids, cytoskeletons, organs, and handedness in humans. Active matter that has chiral symmetry breaking in velocity or shape exhibits rich pattern formation, such as the formation of a large flock assisted by chirality [18] and a chiral edge current [19,20] under spatial constraints that are reminiscent of the quantum Hall effect [21]. Bacteria are also known as chiral active matter; they rotate their flagella in a CCW direction, but the body rotates in a CW direction (when viewed from the back) [22]. When bacteria swim near a solid surface, hydrodynamic interactions between the bacteria and the wall cause a curved trajectory in the CW direction [18]. Hence, bacterial swimming has left–right asymmetry, and bacterial collective motion provides a new platform for studying how the chiral nature of active matter can control the pairing order transition of interacting vortices.

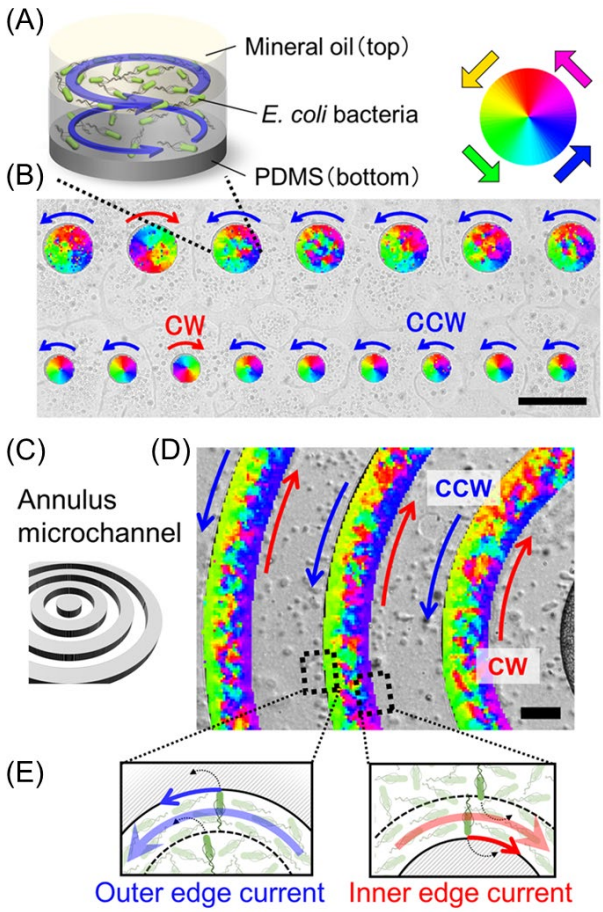

Figure 4 Chiral bacterial vortex and chiral edge current. (A) A schematic illustration of a dense bacterial suspension confined in a microwell with an oil/water interface. (B) The bright-field image of a dense bacterial suspension in circular microwells with 20 μm and 35 μm in radius overlapped by the velocity orientation field. Color codes the orientation. Scale bar, 100 μm. (C) Schematics of the experimental setup of annular microchannels. (D) A bright-field image of a dense bacterial suspension in annular microchannels with 50 μm in width overlaps the velocity orientation field. Color codes the orientation. Scale bar, 50 μm. (E) Schematics of chiral motions near an outer edge and an inner edge. This figure is modified from [23]

Beppu et al. found that it was possible to provide a slight chiral bias on the vertical top–bottom axis while keeping the lateral boundary achiral by sealing a suspension confined in polydimethylsiloxane (PDMS) microwells with oil containing a surfactant [23]. Once a dense bacterial suspension was enclosed in circular microwells with asymmetric interfaces (top: an oil/water interface; bottom: a water/PDMS interface), the suspension started to generate a stable vortex in microwells whose size was comparable to the typical size of vortices (~35 μm) in a turbulent bacterial suspension. The directionality of the emergent vortices was selective, with a ≥95% probability of being CCW when viewed from above (later referred to as the "top view") (Figs. 4A and B). Importantly, persistent chiral collective motion, which is called a chiral edge current, appeared near the lateral boundary (edge layer within 10 μm from the boundary) in relatively large microwells. When a bacterial suspension was confined in concentric microchannels (Fig. 4C), CCW (CW) edge currents occurred at the outer (inner) edge viewed from the center of the annuli. This edge current was stable regardless of the details of the boundary geometry, such as the channel curvature and width (Figs. 4D and E).

Transformation into Global Chiral Vortex

The interplay between the collective motions at the top and bottom interfaces explains the underlying mechanism of the

emergent chiral edge current. Swimming bacteria circle in a CW direction above the surface because of the torque generated by the difference in viscous forces between the surface and bulk side, which act on both the cell body and the helical bundle of flagella (Fig. 5A). In the microwells sealed by a surfactant-laden oil/water interface, bacteria near the bottom PDMS substrate swim in the CW direction (top view). In contrast, bacteria beneath the top oil/water interface swim in the CCW direction because of the high shear caused by the almost no-slip boundary condition of the solid surface (Fig. 5B) [24]. Bacteria interacting with a lateral wall tend to move in one direction owing to the torque caused by flagellar rotation, which leads to effective polar interactions between the bacteria and the lateral wall. In a shallow microwell (height $h \approx 20$ μm), because collective motions at both the top and bottom interfaces are fully correlated throughout the microwell, a coherent rotation between the top and bottom can be generated (Fig. 5C). Although the hydrodynamic interaction between bacteria and a solid interface induces chiral swimming, opposite chiral motions are induced at the top and bottom interfaces in symmetric cylinder microwells, resulting in no net chirality in the bacterial motion. However, the symmetry was broken at the interface where the top surface was the oil/water interface because the bacterial density near the top interface was slightly (~1.2–1.6 times) higher than that at the bottom. Chiral collective motion at the top interface (CCW preference) has a bias in determining the direction of global chirality; hence, robust CCW chiral edge currents can be stabilized without built-in chirality in the boundary condition. One possible reason for the predominance of the top side is that the fluidic oil phase at the top has a higher oxygen content than that of the solid PDMS substrate at the bottom [23]. The preponderance of collective motions at the top in terms of bacterial density suggests that the collective motion at the bottom follows that at the top in the competition between the two interfaces (Fig. 5D). This mechanism of chiral edge currents was verified by a numerical simulation based on the Vicsek-style model, where confined self-propelled particles belonging to two distinct layers (corresponding to the top and bottom) with different densities interact with each other through the coupling strength [23].

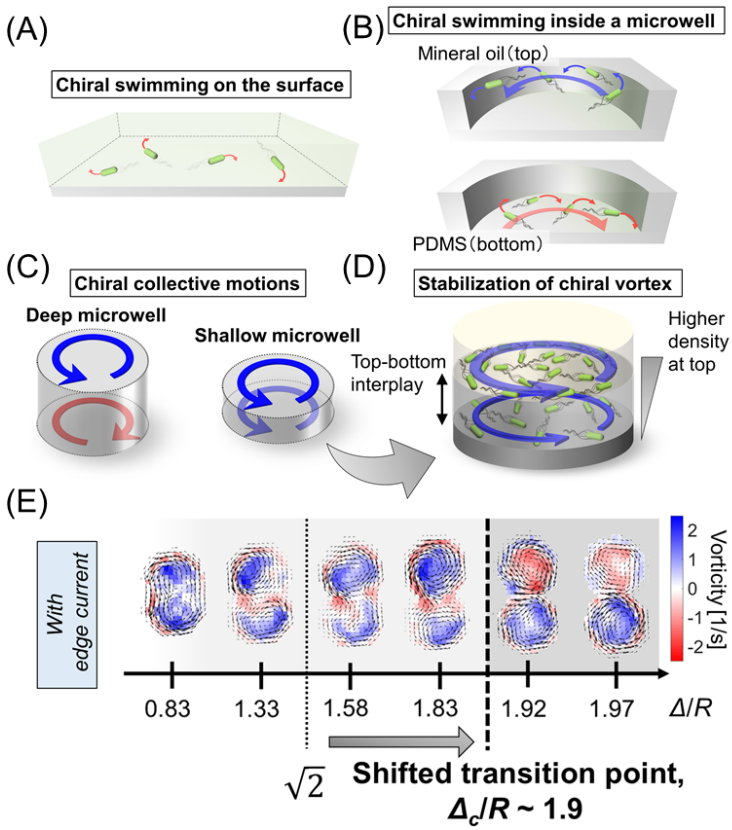

Figure 5 Formation of chiral edge current and chirality-induced FMV pairing. (A) Chiral swimming in CW on the surface in the absence of lateral boundary. (B) Chiral swimming near an oil/water interface and a water/PDMS interface inside a microwell. (C) Chiral collective motions near the interfaces in a deep and a shallow microwell. (D) Schematic model for the formation of chiral edge currents. (E) Geometry dependence of vortex pairings (FMV and AFMV) in microwells with chiral edge current. The dashed line at $\Delta_c/R = \sqrt{2}$ is the transition point of pairing order transition without the edge current. Chiral edge current shifts the transition point to $\Delta_c/R \sim 1.9$. Colors code vorticity. This figure is modified from [23].

Geometric Rule of Interacting Vortices

Edge currents result in large-scale net circulation, suggesting that the chiral edge current controls the interacting ordered vortices inherent in bacterial turbulence. The next question is how such ordered vortices with geometry dependence compete with chiral edge currents seemingly independent of the boundary geometry, or whether the chiral edge current enhances the co-rotational order of interacting vortices.

Beppu et al. predicted the transition point by extending a previous model of self-propelled particles [23]. For microwells with an asymmetric interface, because CCW chiral swimming is selected by the interaction with a boundary wall, the polar interaction toward the CCW direction is incorporated into Equation (1) as follows:

$$\dot{\theta_m} = -\overline{\gamma_p}\sum_{r_{mn}<\varepsilon}\sin(\theta_m - \theta_n) - \overline{\gamma_e}\sum_{r_{mw}<\varepsilon}\sin(\theta_m - \theta_w) + \eta_m(t), \quad (2)$$

where θ_w represents the tangential direction of the wall where the bacteria reach the boundary, and r_{mw} represents the distance from the nearest boundary wall. The second term denotes polar alignment by a chiral edge current at the tip of a doublet circle boundary with $\gamma_e = \sum_{r_{mw}<\varepsilon}\overline{\gamma_e}$. In the same way by taking the geometry of the tip into account, the effective potential of chiral edge currents, i.e., $U_e = -\gamma_e\cos\theta\sin\Psi$, can be obtained. Thus, the transition point is given by the following summation: ${U_p}^{FMV} + U_e|_{\theta=0} = {U_p}^{AFMV} + U_e|_{\theta=\pi/2}$, leading to $(\gamma_p + \gamma_e)\sin\Psi_c = \gamma_p\cos\Psi_c$. Then,

$$\Delta_c/R \approx \sqrt{2}\left(1 + \frac{\gamma_e}{2\gamma_p}\right) \quad (3)$$

is obtained by using the relationship $\Delta_c/R = 2\cos\Psi_c$ and expanding around $\Delta_c/R = \sqrt{2}$. This extended geometric rule predicts the enhancement of the FMV, of which the deviation from $\sqrt{2}$ can be described by the ratio of the strength of the chiral edge current to that of the polar interactions.

To verify the effect of chirality on the pairing order transition, as predicted above, the vortex pairing patterns under the confinement of doublet circular microwells with asymmetric interfaces were examined. Fig. 5E shows an array of vorticity maps overlapped by velocity fields with varying Δ/R values. Enhanced FMV patterns with CCW chirality were observed up to $\Delta_c/R \approx 1.9$. Conversely, the AFMV patterns inherent in bacterial turbulence were maintained even at large Δ/R values and in the presence of robust chiral edge currents. Additionally, a quantitative comparison of γ_e and γ_p between the theory and experiment was performed. This result identified the chiral edge current as a novel phenomenon that governs the pairing-order transition through chirality.

Conclusion and Perspectives

In conclusion, geometrically controlling active-matter systems have unveiled the geometric features of constituent ordered vortices hidden in the chaotic behavior of active turbulence. Meanwhile, bacterial turbulence has intrinsically interacting vortices such as the FMV and AFMV patterns, which are determined by the ratio of the distance between vortices to the radius of the vortices. Despite the apparent geometry dependence of ordered vortices, chiral edge currents suppress the occurrence of an anti-rotational pairing order, allowing us to control a larger flow with net circulation. The theoretical model based on confined self-propelled particles, including an edge current, explains the enhancement of the co-rotational pairing order and provides an extended geometry, where the shift of FMV-AFMV transition point is given by the ratio of an edge current to a local polar alignment. These results may provide a strategy for geometry-based engineering of high-performance micromachines.

This review focused on the geometric control of bacterial collective motion, but the same geometric rule holds for the collective motion of active cytoskeletal systems composed of microtubules and kinesin molecular motors with different orientation interaction symmetries (i.e., nematic interaction) [25]. This implies that the geometry-focused control has a universality that can be applicable to a wide range of active matter. At the interface between physics and biology, there are many unanswered questions regarding the derivation of a generalized rule to uncover the geometric universality of active matter.

Conflict of Interest

The authors declare no conflict of interest.

Author Contributions

K. B. and Y. T. M. wrote the manuscript.

Acknowledgements

This work was supported by a fellowship from Japan Society for the Promotion of Science (grant no. 20J10039 to K.B.) and Grants-in-Aid for Scientific Research on Innovative Areas 16H00805 and 18H05427, Grant-in-Aid for Scientific Research (B) 20H01872, and Grant-in-Aid for Challenging Research (Exploratory) 21K18605 from the Ministry of Education, Culture, Sports, Science and Technology (MEXT) (to Y. T. M.).

References

[1] Vicsek, T., Zafeiris, A. Collective motion. Phys. Rep. 517, 71–140 (2012). https://doi.org/10.1016/j.physrep.2012.03.004
[2] Ramaswamy, S. The mechanics and statistics of active matter. Annu. Rev. Condens. Matter Phys. 1, 323–345 (2010). https://doi.org/10.1146/annurev-conmatphys-070909-104101
[3] Marchetti, M. C., Joanny, J. F., Ramaswamy, S., Liverpool, T. B., Prost, J., Rao, M., et al. Hydrodynamic soft active matter. Rev. Mod. Phys. 85, 1143 (2013). https://doi.org/10.1103/RevModPhys.85.1143
[4] Vicsek, T., Czirok, A., Ben-Jacob, E., Cohen, I., Shochet, O. Novel type of phase transition in a system of self-driven particles. Phys. Rev. Lett. 75, 1226–1229 (1995). https://doi.org/10.1103/PhysRevLett.75.1226
[5] Patteson, A. E., Gopinath, A., Arratia, P. E. The propagation of active-passive interfaces in bacterial swarms. Nat. Commun. 9, 5373 (2018). https://doi.org/10.1038/s41467-018-07781-y
[6] Peng, Y., Liu, Z., Cheng, X. Imaging the emergence of bacterial turbulence: Phase diagram and transition kinetics. Sci. Adv. 7, eabd1240 (2021). https://doi.org/10.1126/sciadv.abd1240
[7] Creppy, A., Praud, O., Druart, X., Kohnke, P. L., Plouraboué, F. Turbulence of swarming sperm. Phys. Rev. E 92, 032722 (2015). https://doi.org/10.1103/PhysRevE.92.032722
[8] Blanch-Mercader, C., Yashunsky, V., Garcia, S., Duclos, G., Giomi, L., Silberzan, P. Turbulent dynamics of epithelial cell cultures. Phys. Rev. Lett. 120, 208101 (2018). https://doi.org/10.1103/PhysRevLett.120.208101
[9] Lin, S-Z., Zhang, W-Y., Bi, D., Li, B., Feng X-Q. Energetics of mesoscale cell turbulence in two-dimensional monolayers. Commun. Phys. 4, 21 (2021). https://doi.org/10.1038/s42005-021-00530-6
[10] Sanchez, T., Chen, D. T. N., DeCamp, S. J., Heymann M., Dogic, Z. Spontaneous motion in hierarchically assembled active matter. Nature 491, 431–434 (2012). https://doi.org/10.1038/nature11591
[11] Linkmann, M., Boffetta, G., Marchetti, M. C., Eckhardt, B. Phase transition to large scale coherent structures in two-dimensional active matter turbulence. Phys. Rev. Lett. 122, 214503 (2019). https://doi.org/10.1103/PhysRevLett.122.214503
[12] Wensink, H. H., Dunkel, J., Heidenreich, S., Drescher, K., Goldstein, R. E., Löwen, H., et al. Meso-scale turbulence in living fluids. Proc. Natl. Acad. Sci. U.S.A. 109, 14308–14313 (2012). https://doi.org/10.1073/pnas.1202032109
[13] Wioland, H., Woodhouse, F. G., Dunkel, J., Kessler, J. O., Goldstein, R. E. Confinement stabilizes a bacterial suspension into a spiral vortex. Phys. Rev. Lett. 110, 268102 (2013). https://doi.org/10.1103/PhysRevLett.110.268102
[14] Wioland, H., Woodhouse, F. G., Dunkel, J., Goldstein, R. E. Ferromagnetic and antiferromagnetic order in bacterial vortex lattices. Nat. Phys. 12, 341–345 (2016). https://doi.org/10.1038/nphys3607
[15] Nishiguchi, D., Aranson, I. S., Snezhko, A., Sokolov, A. Engineering bacterial vortex lattice via direct laser lithography. Nat. Commun. 9, 4486 (2018). https://doi.org/10.1038/s41467-018-06842-6
[16] Beppu, K., Izri, Z., Gohya, J., Eto, K., Ichikawa, M., Maeda, Y. T. Geometry-driven collective ordering of bacterial vortices. Soft Matter 13, 5038–5043 (2017). https://doi.org/10.1039/C7SM00999B
[17] Liu, S., Shankar, S., Marchetti, M. C., Wu, Y. Viscoelastic control of spatiotemporal order in bacterial active matter. Nature 590, 80–84 (2021). https://doi.org/10.1038/s41586-020-03168-6
[18] Lauga, E., DiLuzio, W. R., Whitesides, G. M., Stone, H. A. Swimming in circles: Motion of bacteria near solid boundaries. Biophys. J. 90, 400–412 (2006). https://doi.org/10.1529/biophysj.105.069401
[19] Liebchen, B., Levis, D. Collective behavior of chiral active matter: Pattern formation and enhanced flocking. Phys. Rev. Lett. 119, 058002 (2017). https://doi.org/10.1103/PhysRevLett.119.058002
[20] Liu, P., Zhu, H., Zeng, Y., Du, G., Ning, L., Wang, D., et al. Oscillating collective motion of active rotors in confinement. Proc. Natl. Acad. Sci. U.S.A. 117, 11901–11907 (2020). https://doi.org/10.1073/pnas.1922633117
[21] Bieri, S., Fröhlich, J. Physical principles underlying the quantum Hall effect. C. R. Phys. 12, 332–346 (2011).

https://doi.org/10.1016/j.crhy.2011.02.001
[22] DiLuzio, W. R., Turner, L., Mayer, M., Garstecki, P., Weibel, D. B., Berg, H. C., et al. *Escherichia coli* swim on the right-hand side. Nature 435, 1271–1274 (2005). https://doi.org/10.1038/nature03660
[23] Beppu, K., Izri, Z., Sato, T., Yamanishi, Y., Sumino, Y., Maeda, Y. T. Edge current and pairing order transition in chiral bacterial vortices, Proc. Natl. Acad. Sci. U.S.A. 118, e2107461118 (2021). https://doi.org/10.1073/pnas.2107461118
[24] Lopez, D., Lauga, E. Dynamics of swimming bacteria at complex interfaces. Phys. Fluids 26, 071902 (2014). https://doi.org/10.1063/1.4887255
[25] Araki, S., Beppu, K., Kabir, A. M. R., Kakugo, A., Maeda, Y. T. Controlling collective motion of kinesin-driven microtubules via patterning of topographic landscapes, Nano Lett. 21, 10478–10485 (2021). https://doi.org/10.1021/acs.nanolett.1c03952